Polymer 51 (2010) 1156–1168

Contents lists available at ScienceDirect

Polymer

journal homepage: www.elsevier.com/locate/polymer

Carbon dioxide/ethane mixed-gas sorption and dilation in a cross-linked poly(ethylene oxide) copolymer

Cláudio P. Ribeiro Jr., Benny D. Freeman*

The University of Texas at Austin, Center for Energy and Environmental Resources, 10100 Burnet Road, Building 133, Austin, TX 78758, USA

ARTICLE INFO

Article history:
Received 9 November 2009
Received in revised form
29 December 2009
Accepted 7 January 2010
Available online 15 January 2010

Keywords:
Mixed-gas
Swelling
Solubility

ABSTRACT

Mixed-gas CO_2/C_2H_6 sorption and dilation in a cross-linked poly(ethylene oxide) copolymer were studied at temperatures ranging from −20 to 35 °C. The polymer was prepared by photopolymerization of a solution containing 70 wt.% poly(ethylene glycol) methyl ether acrylate (PEGMEA) and 30 wt.% poly(ethylene glycol) diacrylate (PEGDA). Four different gas mixtures (10, 25, 50 and 70 mol% CO_2) were considered at operating pressures up to 21 atm. At a given temperature, polymer dilation increased with pressure and CO_2 content. Compared to pure-gas values, CO_2 solubility was higher in the presence of ethane, an effect whose extent increased with decreasing temperature. Ethane solubility in the polymer also increased in the presence of CO_2 compared to the pure-gas value at $T \geq 25$ °C. However, at $T \leq 0$ °C, the presence of carbon dioxide initially reduced ethane solubility. As the fugacity of CO_2 in the mixture increased and the polymer dilated, ethane solubility progressively increased, eventually surpassing the pure-gas value. The multicomponent Flory–Huggins model could describe the pure- and mixed-gas data simultaneously, provided that an empirical composition dependence was included in the interaction parameters for $T < 25$ °C.

1. Introduction

There has been a large interest in the development of improved membrane materials for carbon dioxide removal from light gases [1,2], and cross-linked poly(ethylene oxide)s (XLPEOs) are a class of materials studied for this application. These rubbery materials are synthesized from acrylate-functionalized, low molecular weight oligomers, which can be cross-linked, for instance, by exposure to UV light [3–5]. Pure-gas permeability values of dense XLPEO films prepared from a wide variety of oligomers have been reported [6–8]. In particular, copolymers synthesized from poly(ethylene glycol) diacrylate (PEGDA) and poly(ethylene glycol) methyl ether acrylate (PEGMEA) were studied for separation of CO_2/hydrocarbon mixtures in permeation experiments performed with both pure gases and gas mixtures [4,9,10].

Contrary to cellulose acetate and polyimides, the current materials in commercial membranes for CO_2 removal from light gases, XLPEO-based membranes obtain much of their selectivity from high solubility selectivity in favor of CO_2. As a result, characterization of gas solubility in these membranes is of interest. Most of the available gas solubility data for XLPEO materials [7–13] are limited to 35 °C and were obtained neglecting the effect of polymer dilation on sorption, which can lead to errors in the reported solubility values, since experimental methods for measuring gas solubility in polymers are sensitive to the volume of the polymer sample. Recently, Ribeiro and Freeman [14,15] measured both gas sorption and sorptive dilation for two XLPEO materials at different temperatures, reporting, for the first time, gas solubility data in XLPEOs for which the changes in the volume of the polymer sample (due to swelling and thermal expansion) were accounted for. All these previous studies, however, were performed with pure gases, and, to the best of our knowledge, there is still no report on mixed-gas solubility in XLPEOs.

The lack of mixed-gas solubility data is actually a general trend in polymers. Compared to pure-gas sorption, the number of experimental data sets available in the literature for multicomponent sorption in rubbery polymers [16–24] is quite limited. Furthermore, most of these data sets are actually focused on the removal of solvent mixtures from polymers and have been obtained by inverse gas chromatography, which normally imply three limitations for their use in membrane-based gas separation applications: (i) the temperatures at which the data are collected are far above those associated with normal membrane-based gas separation processes, (ii) only ambient pressures are considered, (iii) at least one of the penetrants is present in trace amounts in the gas phase. In rubbery polymers, it is generally supposed, though not necessarily

* Corresponding author. Tel.: +1 512 232 2803; fax: +1 512 232 2807.
E-mail address: freeman@che.utexas.edu (B.D. Freeman).

0032-3861/$ – see front matter © 2010 Elsevier Ltd. All rights reserved.
doi:10.1016/j.polymer.2010.01.012

confirmed, that penetrants sorb independently of one another [25]. This scenario is usually reasonable when the total amount of gas dissolved in the polymer is low, and it was observed, for example, by Joffrion and Glover [16] for *n*-heptane/isopropanol mixtures in atactic polypropylene ($85 \leq T \leq 140$ °C, $P \leq 1.03$ bar). In addition, for toluene/methanol mixtures in poly(vinylacetate) (PVAC) at 60 °C and atmospheric pressure, Surana et al. [18] observed that the infinite dilution solubility of toluene remained constant with increasing concentration of methanol dissolved in the polymer.

Nevertheless, with high levels of gas sorption for at least one component, deviations between pure and mixed-gas solubilities can be observed. For instance, in the polybutadiene/benzene/cyclohexane system, Ruff et al. [17] found that the addition of either penetrant to the vapor phase enhanced the sorption of the other at $60 \leq T \leq 100$ °C. Working with poly(dimethyl siloxane) (PDMS), Raharjo et al. [20] verified that the presence of *n*-butane increased the solubility of methane, while the presence of the later did not affect the solubility of the former in the polymer over a wide range of operating conditions ($-20 \leq T \leq 50$ °C, $3.1 \leq P_{CH4} \leq 16$ atm, $0.07 \leq P_{C4H10} \leq 1.3$ atm). Schabel et al. [19], in turn, reported an increase in methanol vapor solubility in PVAC at 40 °C in the presence of toluene. This latter system was also investigated by Yurekli and Altinkaya [22] at higher temperature (100 °C). The results indicated no effect of toluene on the solubility of methanol in the polymer, whereas the solubility of toluene actually decreased in the presence of methanol. Recently, a decrease in the infinite dilution solubility of ten different vapors (methanol, isopropanol, methyl acetate, benzene, vinyl acetate, ethyl acetate, toluene, ethyl benzene, *p*-xylene) in both PVAC ($40 \leq T \leq 80$ °C) and polystyrene ($130 \leq T \leq 170$ °C) with increasing concentrations of either CO_2 or ethylene dissolved in the polymer was reported [23,24]. Finally, Zielinski et al. [23] verified that the presence of even very small amounts of water dissolved in the polymer was enough to significantly decrease the infinite dilution solubility of toluene in PVAC at 80 °C.

In the particular case of XLPEOs and mixtures containing CO_2, the matter becomes even more complex, since this acid gas exhibits specific interactions with the ether groups in the polymeric chain [26,27]. To the best of our knowledge, there has been no reports probing how such interactions would be affected by the presence of a second gas in the system. Permeation data for CO_2-containing mixtures in XLPEOs are already available, but these reflect combined diffusivity and solubility effects, and any statement specifically concerning the gas–polymer interactions solely based on such data would be speculative.

Therefore, in this contribution, an experimental investigation of mixed-gas solubility and sorptive dilation is reported for the CO_2/C_2H_6 system in an XLPEO prepared by photopolymerization of a PEGDA (30 wt.%) - PEGMEA (70 wt.%) solution. This particular copolymer exhibits high CO_2 permeabilities and good pure-gas selectivity values. Ethane was chosen as the model light gas in view of the large interest in the use of membranes to purify natural gas [2]. Apart from being the second major component of natural gas (after methane), ethane forms a maximum pressure azeotrope with CO_2 that can complicate effective natural gas treatment [28,29]. In addition, due to their similar condensabilities based upon the fact that their critical temperatures are almost the same [30], carbon dioxide and ethane are interesting from a fundamental point of view for an investigation of gas solubility in rubbery polymers. Four different gas mixtures (10,25,50 and 70 mol% CO_2) and five operating temperatures ($-20 \leq T$ (°C) ≤ 35) were evaluated at pressures up to 21 atm.

2. Background

Polymer solution theories have been proposed to describe sorption isotherms in polymeric systems, as discussed in a recent review by Lindvig et al. [31]. In this work, the lattice theory of Flory and Huggins is adopted. Despite its simplifications, it performs remarkably well for a wide variety of polymer-penetrant systems [12,14,15,20,31]. For a ternary system, the Flory–Huggins model is [32,33]:

$$\ln \hat{a}_1 = \ln \Phi_1 + (1-\Phi_1) - \Phi_2\frac{\overline{V}_1}{\overline{V}_2} - \Phi_3\frac{\overline{V}_1}{\overline{V}_3} + (\chi_{12}\Phi_2 + \chi_{13}\Phi_3) \times (\Phi_2 + \Phi_3) - \chi_{23}\frac{\overline{V}_1}{\overline{V}_2}\Phi_2\Phi_3 \quad (1a)$$

$$\ln \hat{a}_2 = \ln \Phi_2 + (1-\Phi_2) - \Phi_1\frac{\overline{V}_2}{\overline{V}_1} - \Phi_3\frac{\overline{V}_2}{\overline{V}_3} + \left(\chi_{12}\Phi_1\frac{\overline{V}_2}{\overline{V}_1} + \chi_{23}\Phi_3\right)(\Phi_1 + \Phi_3) - \chi_{13}\frac{\overline{V}_2}{\overline{V}_1}\Phi_1\Phi_3 \quad (1b)$$

where the index '3' refers to the polymer, '1' and '2' refer to the species dissolving in the polymer, χ_{ij} are interactions parameters between species i and j, Φ_i is the volume fraction of penetrant i in the polymer, $\overline{V}_i$ is the partial molar volume of component i in the polymeric solution, and $\hat{a}_i$ is the activity of species i in the gas mixture in equilibrium with the polymer

$$\hat{a}_i = \frac{\hat{f}_i}{f_i^{sat}} \quad (2)$$

where $\hat{f}_i$ is the fugacity of species i in the gas mixture and f_i^{sat} is the saturation fugacity of the pure-gas i at the operating temperature.

In view of the high molecular weight of the polymer, $\overline{V}_1/\overline{V}_3 \to 0$ and $\overline{V}_2/\overline{V}_3 \to 0$, so that Eq. (1) becomes:

$$\ln \hat{a}_1 = \ln \Phi_1 + (1-\Phi_1) - \Phi_2\frac{\overline{V}_1}{\overline{V}_2} + (\chi_{12}\Phi_2 + \chi_{13}\Phi_3)(\Phi_2 + \Phi_3) - \chi_{23}\frac{\overline{V}_1}{\overline{V}_2}\Phi_2\Phi_3 \quad (3a)$$

$$\ln \hat{a}_2 = \ln \Phi_2 + (1-\Phi_2) - \Phi_1\frac{\overline{V}_2}{\overline{V}_1} + \left(\chi_{12}\Phi_1\frac{\overline{V}_2}{\overline{V}_1} + \chi_{23}\Phi_3\right) \times (\Phi_1 + \Phi_3) - \chi_{13}\frac{\overline{V}_2}{\overline{V}_1}\Phi_1\Phi_3 \quad (3b)$$

Traditionally, gas sorption isotherms are not reported in terms of volume fractions. Instead, the concentration of each gas sorbed in the polymer per unit volume of the corresponding penetrant-free polymer at the operating temperature, C, is used. These two quantities are related as follows:

$$\Phi_i = \frac{C_i\overline{V}_i}{22,414 + \sum_j C_j\overline{V}_j} \quad (4)$$

The Flory–Huggins interaction parameters must be estimated from experimental data. According to their definition, polymer-penetrant interaction parameters depend inversely on temperature and could be composition-independent. Nevertheless, because of the approximate nature of the lattice theory, it is not unusual to include an empirical dependence on solute volume fraction to more accurately represent sorption isotherms of pure penetrants [34]. In principle, χ_{ij} determined from experimental data from the corresponding binary systems can be used to predict sorption isotherms for the ternary system. This procedure is a common practice, for instance, in modeling studies focused on pervaporation [35], with polymer-penetrant interaction parameters (χ_{13} and χ_{23}) determined from pure-liquid sorption data, whereas χ_{12}, the interaction parameter between the two penetrants, is estimated from vapor-liquid equilibrium data using the excess Gibbs energy of mixing, ΔG^E [33,35]:

$$\chi_{12} = \frac{1}{y_1 m_2}\left(y_1 \ln\frac{y_1}{m_1} + y_2 \ln\frac{y_2}{m_2} + \frac{\Delta G^E}{RT}\right) \quad (5)$$

where y_i and m_i are, respectively, the mole and volume fractions of component i in the binary system, and T is the operating temperature. However, in a recent study of multicomponent vapor sorption (toluene + methanol and toluene + *m*-xylene) in PDMS, Lue et al. [21] have demonstrated that the predictions associated with such procedures do not necessarily agree very well with the experimental data.

Alternatives to Eq. (5) have also been considered. In their study of vapor sorption in PVAC at 40 °C using toluene-methanol mixtures, Schabel et al. [19] estimated χ_{12} by fitting the binary Flory–Huggins equation to activity values obtained from liquid–liquid equilibrium data, which required a fourth-order polynomial dependence on penetrant volume fraction and $\chi_{12} \neq \chi_{21}$, giving a total of 10 fitted parameters. Still, significant deviations between predicted and experimental solubilities were found for some operating conditions. For the same ternary system and an operating temperature of 100 °C, Yurekli and Altinkaya [22] estimated χ_{12} from solubility parameters [36], but the agreement between predicted and experimental solubility values was poor, especially for toluene.

On the other hand, a much better quantitative representation of the sorption isotherms is reported when χ_{12} is estimated by directly fitting Eq. (3) to the data set of the ternary system [16,17]. For the benzene (1)/cyclohexane (2)/polybutadiene (3) system, Ruff et al. [17] found that the χ_{12} values fitted from the ternary sorption data were not only different from those estimated from binary vapor-liquid data, but they also showed an opposite temperature dependence.

3. Experimental methodology

3.1. Materials and polymer preparation

Certified ethane-carbon dioxide mixtures (10, 25, 50 and 70 mol% CO_2) were purchased from Praxair Inc. (Danbury, CT). Poly(ethylene glycol) diacrylate (PEGDA; nominal MW = 700 g/mol), poly(ethylene glycol) methyl ether acrylate (PEGMEA, nominal MW = 460 g/mol), and 1-hydroxy-cyclohexyl phenyl ketone (HCPK; 99% purity), the photoinitiator, were obtained from Aldrich Chemical Co. (Milwaukee, WI). All gases and chemicals were used as received.

As detailed in previous studies [9,11,13,37], the copolymer was prepared by adding 0.1 wt.% HCPK to a PEGDA (30 wt.%) - PEGMEA(70 wt.%) solution, stirring for 2 h, placing the resulting solution between two quartz plates, and finally exposing it to 312 nm UV light for 90 s at 3 mW/cm^2 in a UV-cross-linker (Fisher Scientific, model FB-UVXL-1000). The final film was immersed in an ethanol bath for 3 days to remove any residual components or low molecular weight species, and then it was dried at room temperature for at least 7 days. The liquid bath was replaced daily with fresh ethanol. The film thickness, measured with a digital micrometer (Mitutoyo, Model ID-C112E), readable to ± 1 μm, was about 300 μm. At 23 °C, the density of the XLPEO film was 1.153 ± 0.001 g/cm^3, a value determined based on the difference between the weight of three polymer samples in air and in *n*-heptane. According to Lin et al. [9], the glass transition temperature of this material is 216 K.

3.2. Dilation measurements

In the dilation experiments, a strip of the polymer was placed in a temperature-controlled chamber, degassed overnight, and then exposed to a given pressure of the gas mixture under study. With the aid of a COHU (model 491–2000) CCD camera (San Diego, CA), the length of the polymer sample was monitored as a function of time until equilibrium was reached, at which point a further amount of the gas mixture was allowed into the chamber to reestablish equilibrium at a higher pressure. Detailed descriptions of the experimental set-up and procedure are given elsewhere [20,14]. Even though the solubility of the two gases in the polymer is very different, the volume of the dilation chamber was about 700 times larger than the volume of the polymer sample, which insures that any changes in the composition of the gas mixture due to sorption by the polymer sample should be negligible.

Let ΔL_n be the length increase due to gas sorption associated with an equilibrium pressure P_n, l_0 be the length of the polymer sample under vacuum at the operating temperature, and V_0 the volume of the degassed polymer at the same temperature. Assuming isotropic dilation, the change in the polymer volume at P_n (ΔV_n) was calculated by:

$$\frac{\Delta V_n}{V_0} = \frac{V_n - V_0}{V_0} = \left(1 + \frac{\Delta L_n}{l_0}\right)^3 - 1 \quad (6)$$

3.3. Sorption measurements

Gas solubility in the polymer was measured by the barometric pressure-decay method with the same apparatus utilized by Raharjo et al. [20] in their study of mixed-gas sorption in PDMS. It basically comprises three interconnected chambers of known volumes immersed in a temperature-controlled bath, as illustrated in Fig. 1. A known amount of XLPEO film was placed inside the sample chamber, V_2, and degassed at least overnight before beginning an experiment. The charge volume, V_1, initially under vacuum, was then filled with the desired amount of the gas mixture to be tested, and time was allowed for thermal equilibrium to be reached (steady pressure reading). Next, the gas in V_1 was expanded into V_2 and allowed to equilibrate.

In experiments with pure gases, equilibrium is identified by a constant pressure reading over time in V_2. However, in the case of gas mixtures, not only pressure, but also the composition of the gas has to reach its equilibrium value, and each gas expansion into V_2 was followed by a 24-h equilibration time. Then, the analysis volume, V_3, was degassed, and a small amount of the gas in V_2 was expanded into V_3 to be sent to the gas chromatograph (GC) for analysis. More gas mixture was charged into V_1, allowed to reach the operating temperature, and then expanded into V_2. From the

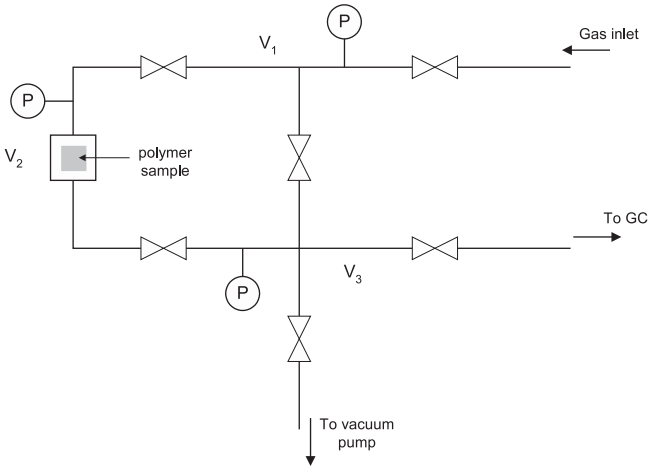

Fig. 1. Set-up for gas sorption experiments: V_1 = charge volume, V_2 = sample volume, V_3 = analysis volume.

second pressure point on, because the gases in V_1 and V_2 necessarily had different compositions, at each expansion, sufficient pressure difference was maintained between these two chambers and the valve connecting them was only slightly opened to minimize diffusional backflow. For each equilibrium point, small amounts of the gas in V_1 were always expanded into V_3 and analyzed in the GC before actually collecting samples from the gas in V_2. To calculate gas solubilities in the polymer, all mass balances were solved using the GC compositions for the gases in V_1 and V_2. Additionally, for each temperature, one mixture was allowed to equilibrate with the polymer for 48 h, and no difference in either the gas composition or pressure in V_2 was found compared to the values obtained for the 24-h equilibration time, indicating that the latter was sufficient to reach equilibrium.

Pressure in each chamber was measured by a Super TJE transducer from Honeywell Sensotec (Columbus, OH), whose accuracy was 0.05% of full scale. The transducer in V_3 had a full scale equal to 100 psia, whereas the full scale of the other transducers was 500 psia. The cell volumes, determined according to the method proposed by Burnett [38], were as follows: $V_1 = 11.58$ cm^3, $V_2 = 15.19$ cm^3, and $V_3 = 11.40$ cm^3. A refrigerated bath circulator (Neslab RTE 140), operating with an aqueous solution of methanol (50 wt.%), provided temperature control. Changes in the gas phase volume of the polymer-containing cell due to sorptive dilation of the polymer sample were taken into account in the mass balances using polynomial equations fitted to the data from dilation measurements (these equations are given in Section 4.1). The effect of temperature on the volume of the gas-free polymer sample was included using the thermal expansion coeffficient of the polymer determined previously [15]. Blank runs without the polymer [12] prove that gas adsorption on the walls of the sorption cells makes a negligible contribution to the observed sorption over the pressure and temperature operating ranges considered in this study.

The pressure-decay method relies on an equation of state (EOS) to transform the pressure readings into a sorption isotherm via mass balances [39,40]. In this contribution, the virial EOS truncated to three terms [41] was adopted. Taking into account that the calculated concentration of gas in the polymer is rather sensitive to small errors in the gas compressibility factor [42], special attention was given to the choice of virial coefficients. For pure carbon dioxide and ethane, we adopted the same coefficients from our previous work [14], which were chosen based on a comparison of density predictions with experimental data for the temperature and pressure ranges of interest. In the case of the mixture, there are not many values of virial coefficients available in the literature for each temperature to choose from, and the values compiled by Dymond et al.[43] were utilized. Details regarding the gas density calculation are given in the Supplementary Material. Density predictions for mixtures were compared with a total of 518 experimental data [44–48] ($260.00 \leq T \leq 323.15$ K, $0.101 \leq P \leq 6.71$ MPa, $0.10043 \leq y_{cd} \leq 0.99$), and the mean prediction error was 0.103%.

4. Results and discussion

4.1. Polymer dilation

Fig. 2 shows the relative change in the volume of the polymer as a function of the total pressure at equilibrium for the different CO_2/C_2H_6 mixtures considered in this work. For comparison, our previous results for the pure gases [15] are also included. Only data related to two temperatures are presented to display the general trends. Dilation data at 35, 0 and −20 °C are recorded in Supplementary Material.

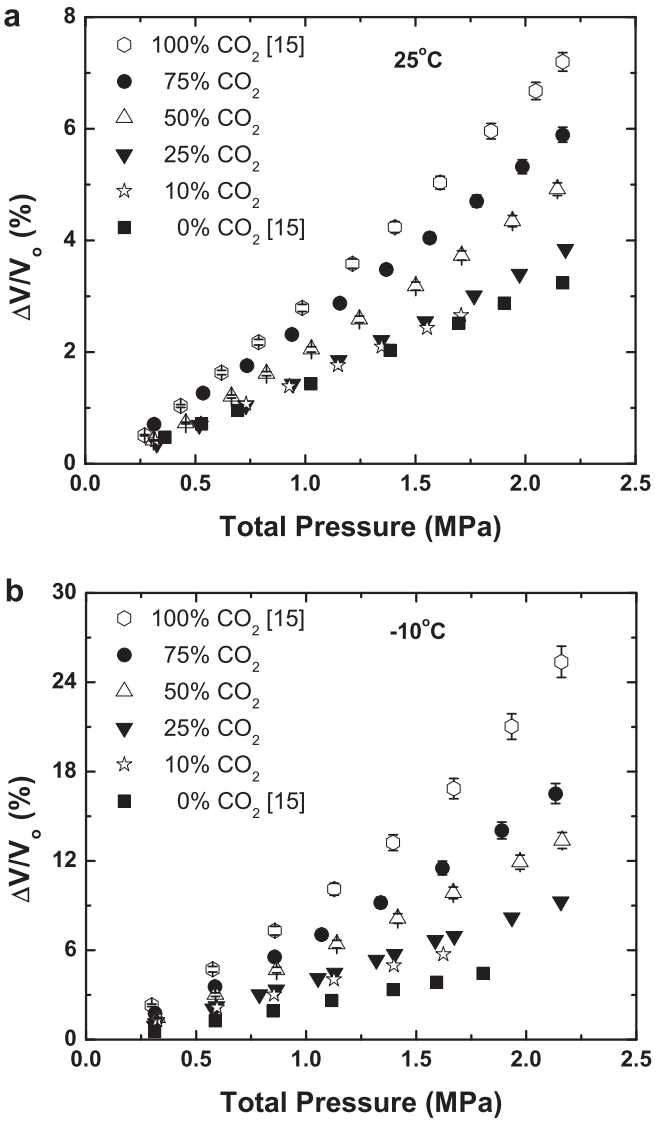

Fig. 2. Sorptive dilation of XLPEO copolymer as a function of equilibrium pressure for different carbon dioxide-ethane mixtures (compositions given in %mol) at 25 °C (a) and −10 °C (b). Pure-gas data from the literature [15] are also shown.

Within the operating range considered, the volume of the polymer always increases with pressure, an effect that becomes progressively more significant as temperature decreases. For instance, at 25 °C, the maximum volume increase was about 7%, whereas volume changes greater than 20% were observed at $T \leq -10$ °C. At the same equilibrium pressure, pure ethane brings about the smallest polymer dilation, whereas pure carbon dioxide causes the largest dilation. The values for the mixtures lie between these two extremes, and for a given pressure, the larger the mole fraction of carbon dioxide in the gas, the higher the polymer dilation. A comparison between Fig. 2(a) and 2(b) shows that the differences among the dilation valules at a given pressure for different gases increase with decreasing temperature. All these trends reflect differences in the amount of gas sorbed by the polymer at a given operating condition, as discussed in Section 4.2.

If the equilibrium pressures and gas compositions during sorption and dilation experiments were always the same, the data from Fig. 2 could be directly used to take the dilation effect into account in the sorption runs. However, such an operational procedure is virtually impossible, and empirical polynomial

equations were fitted to enable the prediction of polymer dilation as a function of operating conditions. Taking into account the non-ideality of carbon dioxide-ethane mixtures, instead of pressure and composition, the data were fitted in terms of gas fugacities, whose values were computed with the virial EOS, as described in the Supplementary Material.

In terms of gas fugacities, at each temperature, one has a dilation surface, as illustrated in Fig. 3 with the 25 °C data. After some trial-and-error tests, the following function was found suitable to represent these surfaces:

$$\frac{\Delta V}{V_0} = c_0 + c_1\hat{f}_{cd} + c_2\hat{f}_{et} + c_3\hat{f}_{cd}^2 + c_4\hat{f}_{et}^2 + c_5\hat{f}_{cd}\hat{f}_{et} \quad (7)$$

in which $\Delta V/V_0$ is given in %, $\hat{f}_{cd}$ and $\hat{f}_{et}$ are the fugacities of carbon dioxide and ethane, respectively, in the mixture, and c_0 to c_5 are temperature-dependent constants. The values of c_0 to c_5 for each temperature were obtained by multiple linear regression of the dilation data and are recorded in Table 1. For qualitative accessment, the predictions of Eq. (7) are shown as a wire surface in Fig. 3, and the good agreement is apparent. To put such agreement into a quantitative perspective, the regression coefficients ($\Re^2$) associated with each data fit are listed in Table 1. The values are all rather close to unity, confirming the quality of the fit. Pure-gas data were included in the regression (by considering the pure-gas i as a mixture with $y_i = 1$) and are, therefore, also represented by Eq. (7).

4.2. Gas sorption

4.2.1. Comparison between pure- and mixed-gas solubility

Fig. 4 presents sorption isotherms obtained with carbon dioxide/ethane mixtures at −10 °C. Due to the addition of the actual mixtures into the polymer-containing volume during the sorption experiments, instead of only pure gases as done in previous studies [20,49,50], the fugacity of both gases varies simultaneously during the experiment as pressure is increased. Consequently, instead of sorption curves for gas i at an approximately constant fugacity of gas j, our experimental procedure leads to sorption surfaces for each gas, as illustrated in Fig. 4. The advantages of this procedure are twofold. First, it enables one to obtain the sorption surface in a given domain of gas fugacities with a fewer number of experiments, and second, it minimizes the risk of diffusional backflow into the charge volume during the runs.

The trends seen in Fig. 4 are representative of those observed at the other operating temperatures. At a given T, the concentration of each gas dissolved in the polymer increased smoothly as pressure, and, therefore, the fugacities of carbon dioxide and ethane in the mixture, increased. This trend highlights the important dependence of our experimental sorption values on the fugacity of both

Table 1
Constants for the estimation of XLPEO dilation due to gas sorption in the carbon dioxide-ethane system using Eq. (7) and regression coefficients ($\Re^2$) of each fitting.

T (°C)	$c_0 \times 10$	$c_1 \times 10$ (atm^{-1})	$c_2 \times 10$ (atm^{-1})	$c_3 \times 10^2$ (atm^{-2})	$c_4 \times 10^3$ (atm^{-2})	$c_5 \times 10^2$ (atm^{-2})	$\Re^2$
35	−0.21288	2.12960	1.19238	0.41415	1.65270	0.52027	0.9992
25	−1.15151	2.53159	1.38603	0.69153	2.42882	0.48910	0.9972
0	−7.57833	6.33231	3.64518	1.25214	−2.96235	0	0.9999
−10	2.24308	5.05108	2.21773	4.71159	6.97609	2.86740	0.9964
−20	2.64185	4.87493	2.95432	8.69051	0	6.97278	0.9975

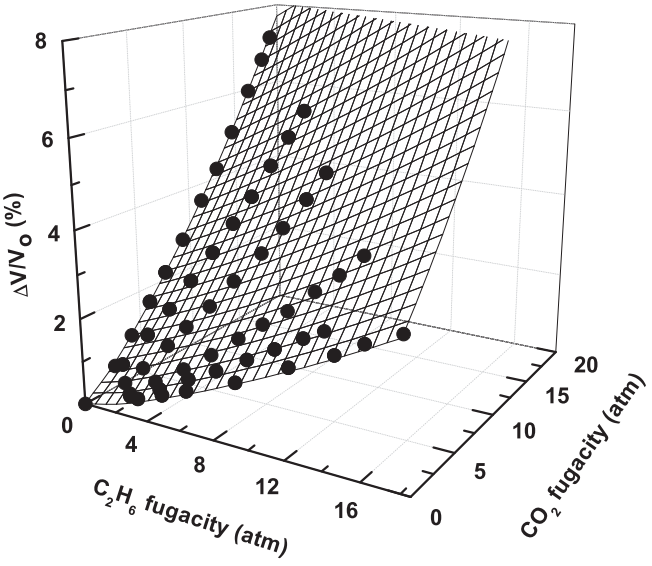

Fig. 3. Sorptive dilation of XLPEO copolymer as a function of gas fugacity for the carbon dioxide-ethane system at 25 °C. The wire surface is the prediction of Eq. (7) with the constants given in Table 1.

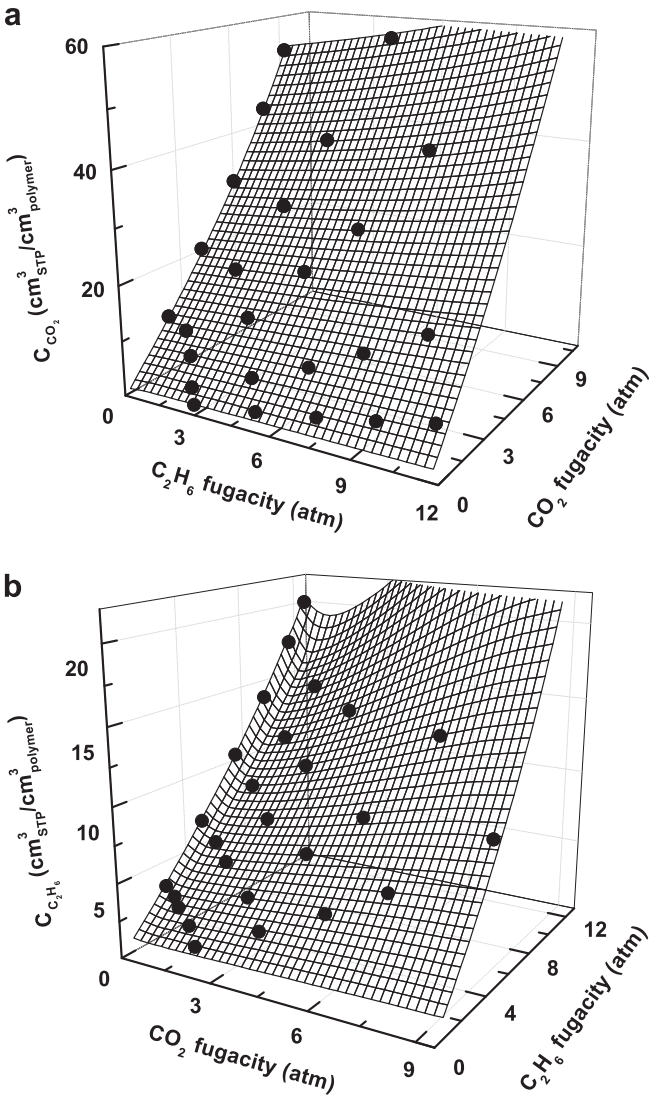

Fig. 4. Mixed-gas sorption isotherms for (a) carbon dioxide and (b) ethane in XLPEO copolymer as a function of the fugacity of each gas in the mixture at −10 °C. In each graph, the corresponding pure-gas sorption data [15] are also included. The wire surface is the prediction of the multicomponent Flory–Huggins model with the parameters fitted in this work.

gases in the mixture. Nonetheless, there is a clear limitation in this way of presenting the data. Even though the pure-gas sorption data from our previous work [15] are also included in Fig. 4, it is very difficult to recognize if there are any differences between the pure- and mixed-gas solubility of each gas due to the subtleties of the three-dimensional representation.

To overcome this limitation, mixed-gas sorption data for carbon dioxide and ethane at two different temperatures (25.0 and −10.0 °C) are presented in Figs. 5 and 6 as two-dimensional plots. Similar pictures showing the data related to the other temperatures considered in this work (35.0, 0.0 and −20.0 °C) can be found in the Supplementary Material. In these pictures, the gas solubility in the polymer ($S_i = C_i/\hat{f}_i$) is plotted as a function of fugacity. In each plot, the data are labeled according to the *initial* composition of the mixture that was in the charge volume (V_1 in Fig. 1). Tables containing all sorption data obtained in this study are found in the Supplementary Material.

From Fig. 5, the presence of ethane can increase the solubility of carbon dioxide in the polymer. At a given temperature, for sufficiently low values of CO_2 fugacity, pure- and mixed-gas solubility values are similar, but the size of this fugacity range is considerably reduced as the content of ethane in the mixture increases and/or the temperature is reduced. Once this fugacity range is surpassed, the carbon dioxide solubility in the polymer is not only higher for the mixture, but it also increases at a higher rate with carbon dioxide fugacity. Overall, the effect of ethane on CO_2 solubility is not very pronounced at temperatures around ambient, as illustrated in Fig. 5(a) by the data at 25 °C (and by the data at 35 °C in the Supplementary Material). Nevertheless, the same is not true at low temperatures ($T \leq 0$ °C), as shown by the data at −10 °C in Fig. 5(b), in which case an increase of up to about 40% in the mixed-gas solubility was observed compared to the pure-gas value at the same CO_2 fugacity.

The effect of carbon dioxide on ethane solubility in the polymer is more complex. At 25 °C, ethane solubility values obtained with the mixtures containing 25 and 10 mol% CO_2 are not different from their pure-gas values over the range of ethane fugacities considered. On the other hand, higher ethane solubility in the polymer for the mixed-gas experiments becomes evident for the mixture containing 50 mol% CO_2, an effect which is even more pronounced in

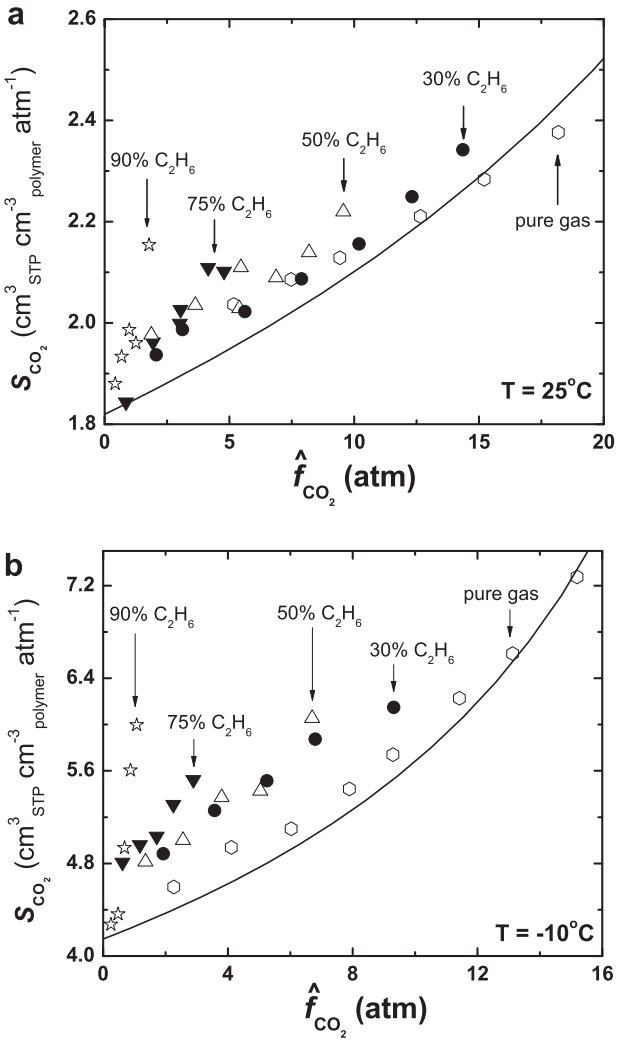

Fig. 5. Carbon dioxide solubility in XLPEO copolymer as a function of fugacity for pure CO_2 [15] and four different ethane-carbon dioxide mixtures. Mixed-gas data are labeled according to the initial composition (in mol%) of the mixture that was in the charge volume (V_1 in Fig. 1). Data are presented from two temperatures: (a) 25.0 and (b) −10.0 °C. The lines are predictions of the pure-gas solubility from the Flory–Huggins model [15].

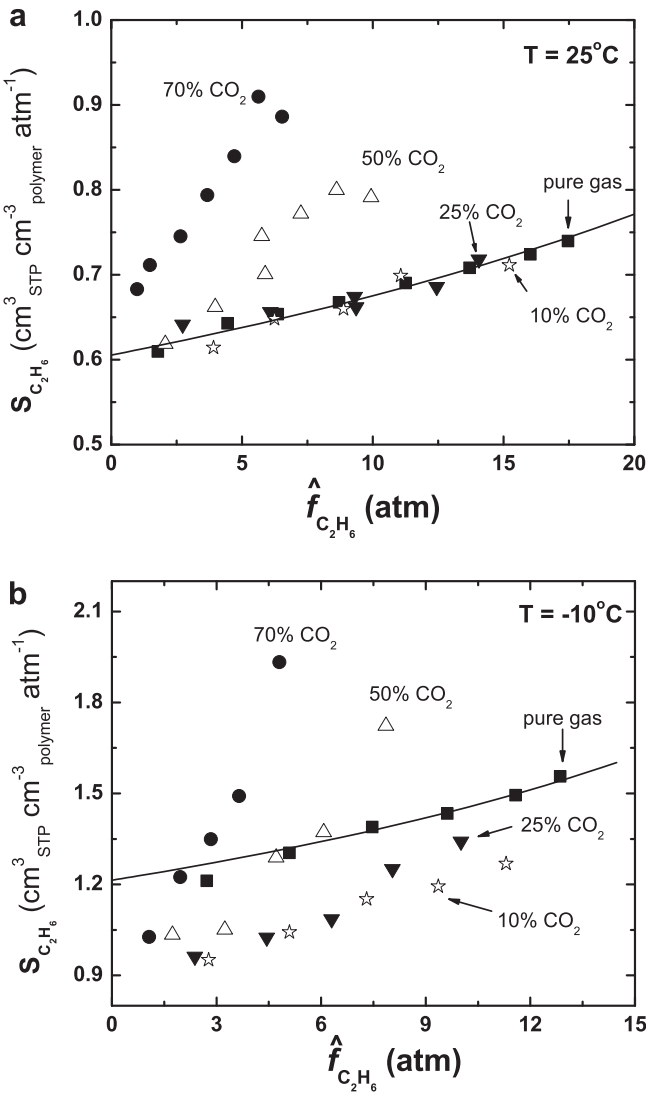

Fig. 6. Ethane solubility in XLPEO copolymer as a function of fugacity for pure ethane [15] and four different ethane-carbon dioxide mixtures. Mixed-gas data are labeled according to the initial composition (in mol%) of the mixture that was in the charge volume (V_1 in Fig. 1). Data are presented from two temperatures: (a) 25.0 and (b) −10.0 °C. The lines are predictions of the pure-gas solubility from the Flory–Huggins model [15].

the mixture containing 70 mol% CO_2. A similar trend was also observed at 35 °C, as shown in the Supplementary Material. In Fig. 6(b), a new aspect is revealed: ethane solubility in the polymer measured with all mixtures is initially lower than the pure-gas value. For mixtures containing 50 and 70 mol% CO_2, ethane solubility reaches the pure-gas value at an ethane fugacity below 5 atm, from which point on the mixed-gas solubility becomes higher than the pure-gas one. For the other two mixtures, with 25 and 10 mol% CO_2, the mixed-gas solubility of ethane in the polymer remains lower than the pure-gas value over the entire pressure range. This unexpected and complex trend is confirmed by data at 0 and −20 °C presented in the Supplementary Material. In particular, at −20 °C, the ethane solubility in the polymer for the mixtures containing 25 mol% CO_2 or less can be less than about half the pure-gas value obtained at the same fugacity.

The data in Figs. 5 and 6 illustrate that the general hypothesis that penetrants sorb independently of one another in rubbery polymers has a rather limited range of application.

4.2.2. Fitting of Flory–Huggins parameters

Before rationalizing the trends in the mixed-gas sorption data, we focus on the mathematical description of these data using the multicomponent Flory–Huggins model. To accurately predict the solubility of each gas in the polymer at a given operating condition and mixture composition, the interaction parameters in Eq. (3) were fitted using both binary and ternary sorption data. Initially, interaction parameters were considered to be composition-independent, but this led to a poor representation of the isotherms for $T \leq 0$ °C. Different empirical expressions were tested to include in χ_{ij} a dependence on the solute volume fraction, and the following equations were found suitable:

$$\chi_{13} = \delta^{\infty} + \delta^{*}\Phi_2 \tag{8a}$$

$$\chi_{23} = \beta^{\infty} + \beta^{*}\sqrt{\Phi_1} \tag{8b}$$

$$\chi_{12} = \gamma^{\infty} + \frac{\gamma^{*}}{\ln \Phi_1} \tag{8c}$$

where the indices '1', '2', and '3' refer to carbon dioxide, ethane, and the polymer, respectively. The parameters δ^{∞}, δ^{*}, β^{∞}, β^{*}, γ^{∞}, and γ^{*} are empirical constants to be fitted. One should note that, in the limit of infinite dilution ($\Phi_1 \to 0$ and $\Phi_2 \to 0$), these empirical expressions tend towards a constant value, in agreement with the original Flory–Huggins theory. Power series, such as Eq. (8a), are normally used to represent the concentration dependence of polymer-penetrant interaction parameters [12,19,51]. With regard to the penetrant–penetrant interaction parameter, even though Eq. (8c) is empirical, it was proposed based on an analysis of χ_{12} values calculated from Eq. (5) for carbon dioxide(1)-ethane(2) mixtures using the Peng-Robinson EOS to predict ΔG^{E}, as detailed in the Supplementary Material.

At each temperature, the empirical constants in Eq. (8) were fitted using the maximum likelihood method [52] considering all pure- and mixed-gas sorption data simultaneously. In these data regressions, the partial molar volume of each gas as a function of temperature was calculated as described previously [15]. The parameters are listed in Table 2. Also included in this table are the average prediction errors for the concentration of gas dissolved in the polymer, whose small values indicate the adequacy of the fit. To put the predictive character of these fittings into a more visual perspective, parity plots for the data sets associated with the lowest (25 °C) and highest (−20 °C) mean prediction errors are given in Fig. 7. In both cases, the points lie very close to the $y = x$ line and are randomly scattered around it. Furthermore, as a final assessment of the fitting, the computed isotherms at −10 °C are shown in Fig. 4 as a wire surface. Once again, good agreement between experimental and calculated equilibrium concentrations is observed.

4.2.3. Analysis of mixed-gas effects

Among the limited number of studies on mixed-gas sorption in rubbery polymers, there is little discussion of the physical explanation for the observed differences in solubility between the binary and ternary systems. Most often, only general remarks involving the miscibility of the penetrants with each other are made [16]. These work well to justify monotonic trends, such as an increase in the solubility of benzene in polybutadiene in the presence of cyclohexane (and vice versa) [17], or a decrease in the solubility of toluene in PVAC in the presence of water [23]. However, the same ideas can not explain the complex trends observed for our system, since carbon dioxide can either decrease or increase ethane solubility, depending on the operating temperature or pressure. Moreover, examples of a solubility decrease in systems of two penetrants with good miscibility [23,24], as well as a solubility increase in systems of two penetrants with limited miscibility [19], have been reported.

For the methane/*n*-butane/PDMS system, Raharjo et al. [20] verified that the increase in methane solubility due to the presence of *n*-butane could be well described by the thermodynamic model of gas dissolution in mixed solvents developed by O'Connell and Prausnitz [53], considering *n*-butane and PDMS as the individual solvents. This model assumes that only two-body interactions contribute significantly to the excess free energy of the ternary mixture and that the characteristic coefficients for these interactions are given by empirical constants determined from binary data. Even though this model provides a good approximation for solutions of nonpolar molecules, both positive and negative deviations from its predictions have already been observed for a single solute in binary liquid mixtures when polar molecules are present [54–57]. Besides, contrary to the case of methane/*n*-butane mixtures, there is no clear choice for the second solvent in the case of carbon dioxide/ethane mixtures, since both gases have similar condensability and form close boiling mixtures over the entire range of compositions [58–61].

In an attempt to provide some insight into the reasons behind the complex trends in our mixed-gas sorption data, in Fig. 8, mixed-gas ethane solubility in XLPEO at 25 and −10 °C is plotted as a function of the amount of carbon dioxide dissolved in the

Table 2
Parameters for the calculation of gas solubility in XLPEO copolymer(3) for the system carbon dioxide(1)-ethane(2) using Eqs. (3) and (8). Values with standard deviations were determined by the maximum likelihood method using pure- and mixed-gas sorption data, while values without standard deviations were specified and held constant.

T (°C)	Number of data points	δ^{∞} (−)	δ^{*} (−)	β^{∞} (−)	β^{*} (−)	γ^{∞} (−)	γ^{*} (−)	Av. Pred. Error (%)[a]
35.0	72	0.8877 ± 0.0048	0	1.9783 ± 0.0071	0	1.75 ± 0.24	0	3.04
25.0	78	0.9085 ± 0.0036	0	2.0804 ± 0.0061	0	1.52 ± 0.16	0	2.17
0.0	94	0.9686 ± 0.0036	7.5 ± 1.4	2.310 ± 0.012	2.86 ± 0.38	−18.0 ± 2.9	−32.1 ± 5.5	3.85
−10.0	70	1.0421 ± 0.0045	12.3 ± 2.1	2.421 ± 0.015	4.76 ± 0.50	−28.2 ± 4.2	−44.3 ± 8.2	3.78
−20.0	56	1.0665 ± 0.0076	24.2 ± 3.0	2.476 ± 0.021	9.52 ± 0.76	−59.0 ± 6.1	−93 ± 11	6.54

[a] The average prediction error was calculated as $\sum_{i=1}^{n} |(C_i^{\text{pred}} - C_i^{\text{exp}})|/C_i^{\text{exp}} \times 100$, where n is the number of experimental data.

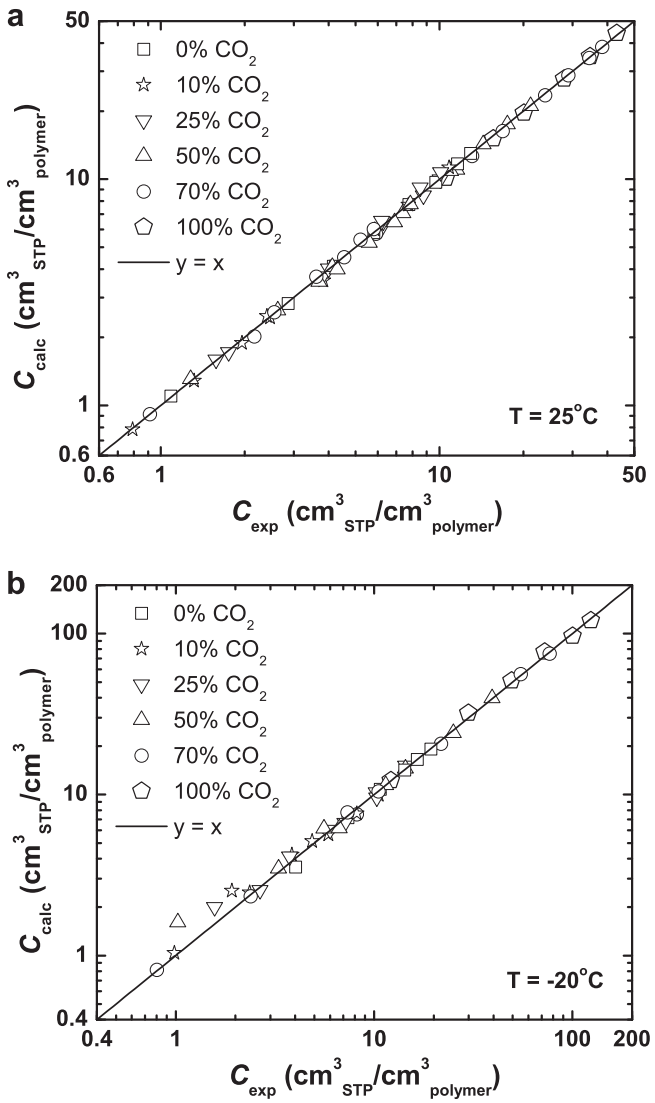

Fig. 7. Comparison between experimental and calculated values for the concentrations of gas dissolved in XLPEO copolymer in equilibrium with carbon dioxide, ethane, and their mixtures at 25 °C (a) and −20 °C (b). Concentrations were calculated with Eqs. (3) and (8) and the parameters listed in Table 2. Each graph has the $y = x$ line plotted as a reference.

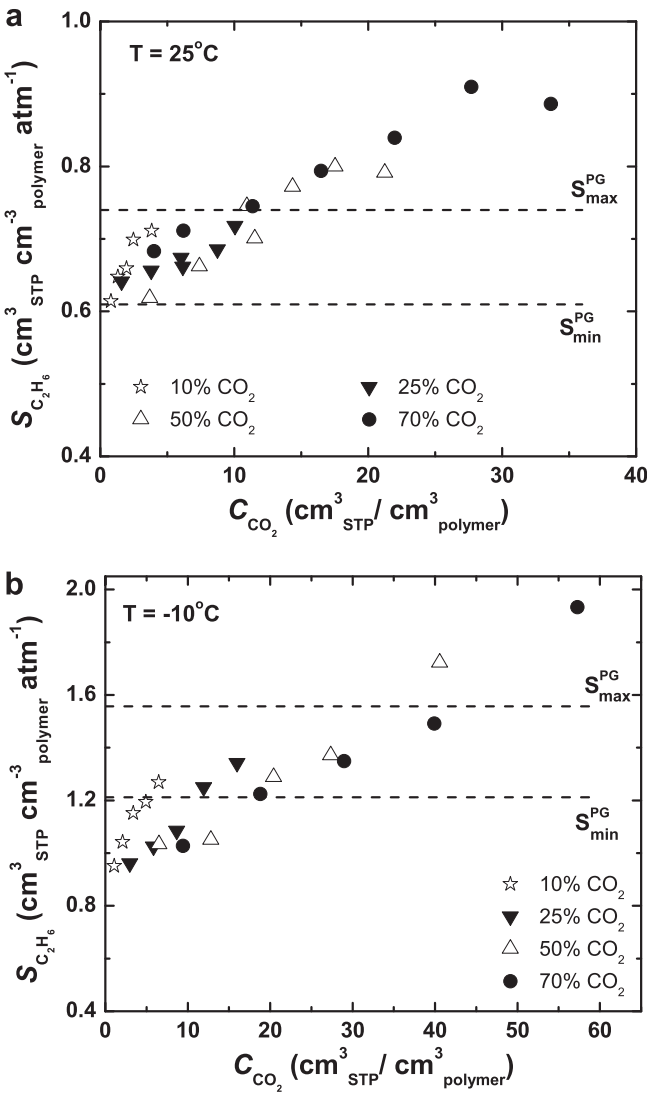

Fig. 8. Mixed-gas ethane solubility in XLPEO copolymer as a function of the amount of carbon dioxide dissolved in the polymer at (a) 25.0 and (b) −10.0 °C. Data are labeled according to the initial composition (in mol%) of the mixture that was in the charge volume (V_1 in Fig. 1). The dashed lines indicate the range of pure-gas solubility values, where S^{PG}_{min} and S^{PG}_{max} are, respectively, the lowest and highest pure-gas solubility measured at a given temperature.

polymer. Regardless of the operating temperature, ethane solubility increases with increasing carbon dioxide concentration in the polymer. The difference lies in the region of low carbon dioxide content. At 25 °C, mixed-gas data in this region converge to the pure-gas value, whereas, at −10 °C, mixed-gas solubility values lie considerably below the pure-gas region. Although the data sets related to different gas compositions are much closer than when plotted as a function of ethane fugacity (Fig. 6), they still do not lie in the same curve.

Because of the experimental procedure, solubility data in Fig. 8 for a given carbon dioxide concentration are associated with different values of ethane activity. In Section 4.2.2, it was demonstrated that the multicomponent Flory–Huggins model properly represents the sorption data with the parameters fitted in this work. Thus, to further explore the aspects revealed in Fig. 8, Eq. (3) was used to compute the solubility of ethane in the polymer as a function of the fugacity of carbon dioxide in the mixture for a fixed ethane activity in the gas phase. The results are presented in Fig. 9. The unexpected difference seen in Fig. 8 between the data set at 25 and −10 °C is now clear. Regardless of the operating temperature, all isotherms in Fig. 9(a) converge to the pure-gas value as the amount of carbon dioxide dissolved in the polymer goes to zero, but a monotonic increase in ethane solubility with the carbon dioxide content in the polymer is only observed at 25 and 35 °C. At 0 °C and below, ethane solubility displays a minimum at low carbon dioxide concentrations. As shown in Fig. 9(b), at a given temperature, the general shape of the solubility curves does not depend on ethane activity, but for the same concentration of CO_2 dissolved in the polymer, a higher ethane activity leads to a higher solubility. This trend explains why the data for different gas compositions do not lie on a single curve in Fig. 8(b). As ethane content in the gas phase increases, to obtain the same CO_2 concentration in the polymer, the total pressure must increase, which implies a higher ethane activity. Accordingly, in Fig. 8, ethane solubility for a given CO_2 concentration in the polymer is normally higher for the mixtures whose initial ethane content in the charge volume was higher.

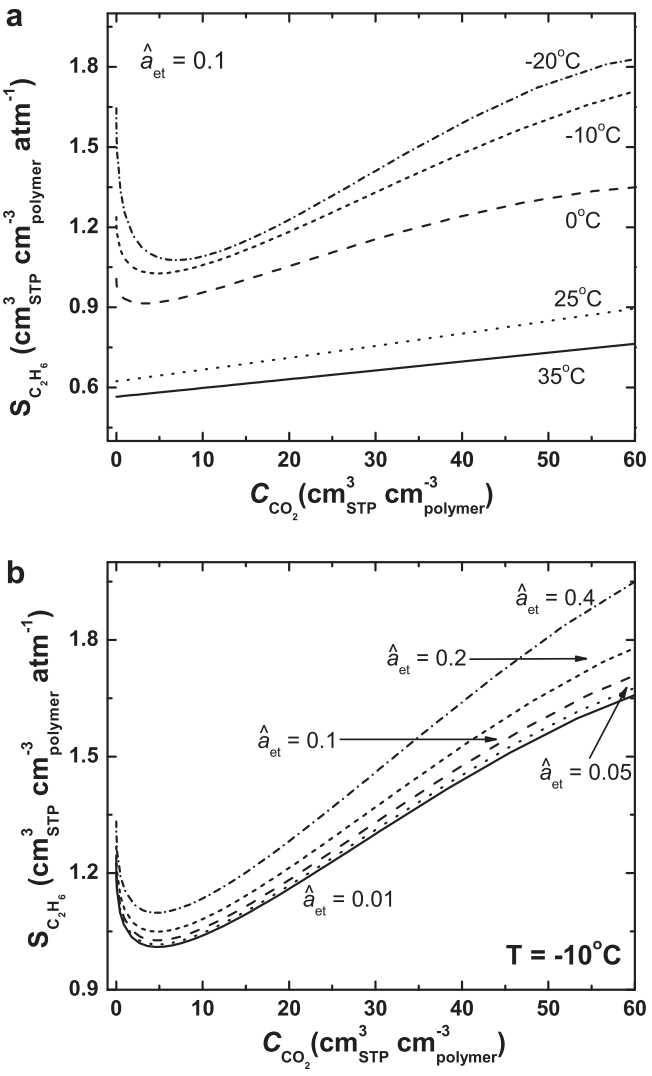

Fig. 9. Mixed-gas ethane solubility in XLPEO copolymer as a function of the amount of carbon dioxide dissolved in the polymer at fixed ethane activity ($\hat{a}_{et}$): (a) effect of operating temperature for $\hat{a}_{et} = 0.1$; (b) effect of ethane activity at $T = -10$ °C. All values were calculated with the multicomponent Flory–Huggins model using the interaction parameters in Table 2.

To the best of our knowledge, the appearance of a minimum in the solubility of a gas in a rubbery polymer for a ternary system with decreasing temperature has not been previously reported. At present, we do not have a definitive explanation for this complex behavior. It is important to highlight, however, that a similar trend is well documented in the literature for the dissolution of inert gases (helium, hydrogen, oxygen, argon) in water + alcohol (methanol, ethanol, *n*-butanol) mixtures [62–65]. Although alcohols are better solvents than water for inert gases, the gas solubility against alcohol mole fraction curves do not exhibit a monotonic increase. Instead, in the low alcohol concentration range, an inflection point is observed at temperatures around 25 °C or higher, whereas a maximum and then a minimum are found at lower temperatures. Initially, these phenomena in aqueous systems were explained in terms of a 'two-structure' model for liquid water. This model assumes the existence of a thermodynamic equilibrium between monomeric water molecules and hydrogen-bonded water clusters, an equilibrium that is shifted by the introduction of the inert gas. However, it was later argued [66] and recently proven by molecular simulation [67–69] that structural reorganization of the solvent is enthalpy-entropy compensating and, therefore, should not have any effect on solubility. Thus, even in low molar mass systems, the molecular mechanism responsible for such complex trends in solubility remains unclear.

4.2.4. Effect of temperature

Further insight into the complex behavior observed in the mixed-gas data can be obtained by analyzing the effect of temperature on gas solubility. Traditionally, this is accomplished by defining an enthalpy of sorption using the solubility at the limit of infinite dilution, and gas sorption is viewed as a two-step thermodynamic process involving gas condensation and subsequent mixing of the hypothetic fluid with the polymer [70]. More recently, however, van der Vegt [71,72] proposed an alternative framework to examine gas dissolution in polymers in the limit of infinite dilution, and this framework will be used here. It is based on modern theories of solvation thermodynamics and molecular simulation methods. Gas sorption is still viewed as a two-step process, but the steps are the creation of a cavity in the polymer matrix to accommodate the solute and the inclusion of the solute in this cavity. Thus, the enthalpy of sorption, ΔH_S, as well as the entropy and the Gibbs energy of sorption, is a sum of the contributions related to polymer reorganization (step I) and binding interactions of the gas with the polymer (step II).

In this case, the isosteric enthalpy of sorption, that is, the enthalpy of sorption of penetrant *i* at a given volume fraction of penetrant *j* in the polymer ($\Delta H_{S,i}^{\Phi_j}$), is calculated and reported. The value of $\Delta H_{S,i}^{\Phi_j}$ is obtained from the Ostwald solubility coefficient at infinite solution [71,72]:

$$\frac{\Delta H_{S,i}^{\Phi}}{R} = -\left(\frac{\partial \ln \Omega_{\infty,i}}{\partial(1/T)}\right)_{\Phi_j} \tag{9}$$

The Ostwald solubility coefficient is related to the infinite dilution solubility of the gas in the polymer, S_∞, as follows [73]:

$$\Omega_\infty = \frac{TS_\infty P^o}{T^o} \tag{10}$$

where T° and P° are the standard temperature (273.15 K) and standard pressure (1 atm), respectively.

At each temperature, the solubility of the gas in the polymer was computed from the multicomponent Flory–Huggins equation, which, in the limit of infinite dilution, simplifies to:

$$S_{\infty,1} = \frac{22,414}{\overline{V}_1 f_1^{sat}(1-\Phi_2)} \exp\left[\Phi_2\left(\frac{\overline{V}_1}{\overline{V}_2} - \chi_{12}\right) + (1-\Phi_2)\left(\chi_{23}\frac{\overline{V}_1}{\overline{V}_2}\Phi_2 - \chi_{13}\right) - 1\right] \tag{11a}$$

$$S_{\infty,2} = \frac{22,414}{\overline{V}_2 f_2^{sat}(1-\Phi_1)} \exp\left[\Phi_1\frac{\overline{V}_2}{\overline{V}_1}(1-\chi_{12}) + (1-\Phi_1)\left(\chi_{13}\frac{\overline{V}_2}{\overline{V}_1}\Phi_1 - \chi_{23}\right) - 1\right] \tag{11b}$$

For each temperature considered in this work, Ostwald solubility coefficients of each gas were calculated at different volume fractions of the other penetrant in the polymer. Some results are presented in Fig. 10, and there is an effect of the presence of one gas on the infinite dilution solubility of the other gas in polymer. For carbon dioxide, $\ln \Omega_\infty$ varied linearly with $1/T$ for all concentrations of ethane in the polymer, indicating that the isosteric enthalpy of sorption was not a function of temperature. A total of 18 Φ_{et} values were considered, and the average $\Re^2$ for the linear regressions to

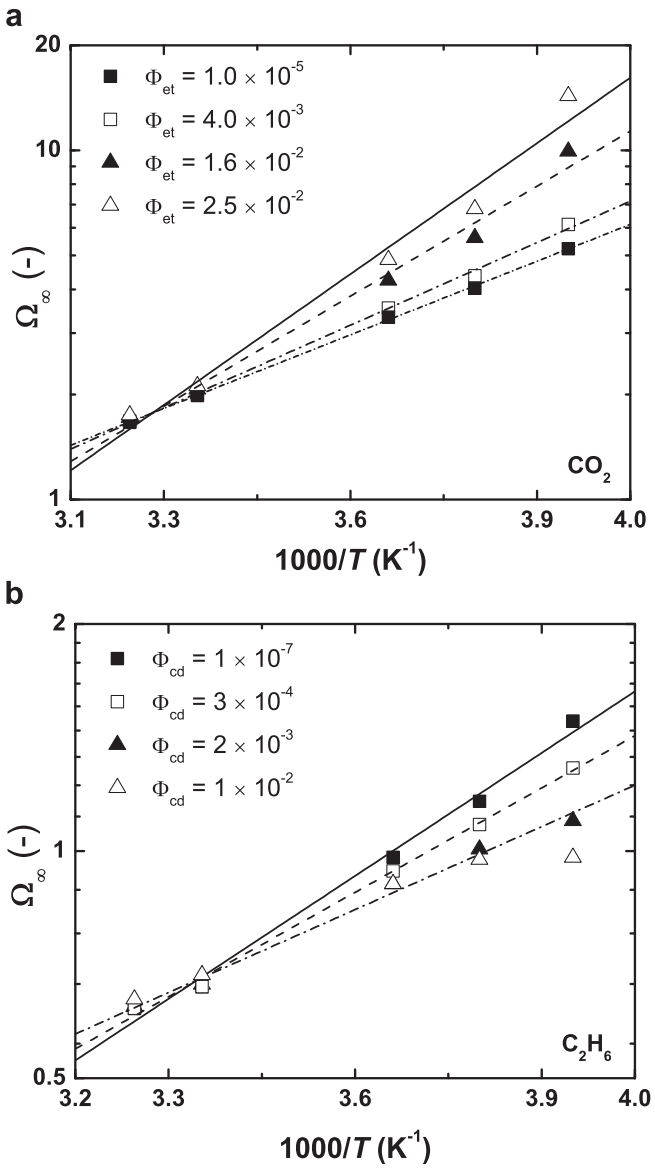

Fig. 10. Infinite dilution Ostwald solubility coefficients of (a) carbon dioxide and (b) ethane at a given volume fraction of the other component in the polymer. Each line corresponds to a least-square fit of the data at a given Φ to Eq. (9).

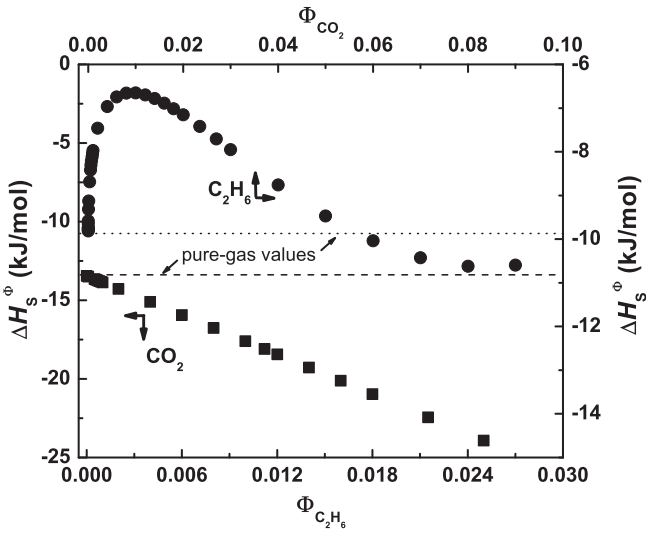

Fig. 11. Isosteric enthalpy of sorption for carbon dioxide and ethane in XLPEO copolymer as a function of the volume fraction of the other component in the system. The lines represent the values calculated based on pure-gas sorption data.

obtain $\Delta H_{S,cd}^{\Phi}$ was 0.9939. This linear behavior was also observed for ethane over the entire temperature range for $\Phi_{cd} \leq 6 \times 10^{-3}$, but further increases in Φ_{cd} restricted the linear dependence of $\ln \Omega_\infty$ on $1/T$ to the range $-10 \leq T\,(^\circ C) \leq 35$. For $\Phi_{cd} > 6 \times 10^{-3}$, the solubility coefficient of ethane at −20 °C became progressively smaller than the value predicted by the linear trend based on the data for the other temperatures. This is illustrated in Fig. 10(b) by the data for $\Phi_{cd} = 1 \times 10^{-2}$, in which there is little difference between the $\Omega_{\infty,et}$ values at the two lowest temperatures. Unfortunately, we only have data for one temperature lower than −10 °C, and the changes in $\Omega_{\infty,et}$ could not be converted into $\Delta H_{S,et}^{\Phi}$ values in this region.

Fig. 11 shows the isosteric enthalpy of sorption of each gas as a function of the volume fraction of the other species in the polymer. For comparison, the values calculated from pure-gas data [15] are also plotted. Due to the reasons pointed out in the previous paragraph, the values for ethane are reported at $-10 \leq T\,(^\circ C) \leq 35$.

Starting with CO_2, the enthalpy of sorption becomes systematically more negative as ethane volume fraction increases. That is, as the concentration of ethane in the polymer increases, the sorption of carbon dioxide (extrapolated to infinite dilution) becomes more exothermic. One could interpret these results as evidence that the interactions of CO_2 with the polymer were favored by the presence of ethane, which would then explain the higher mixed-gas CO_2 solubility compared to the pure-gas value. Nevertheless, it should be born in mind that the enthalpy of sorption is composed of two terms [71]:

$$\Delta H_S = \Delta u_{vv} + \Delta u_{uv} \tag{12}$$

where Δu_{vv} is an endothermic contribution related to polymer reorganization and Δu_{uv} is an exothermic term associated with polymer-penetrant interactions. At this point, without results from molecular dynamics simulation, it is impossible to determine how much of the reduction in $\Delta H_{S,cd}^{\Phi}$ with increasing Φ_{et} is actually due to an increase in the absolute value of Δu_{uv} and how much comes simply from a reduction in Δu_{vv}.

The variation in ethane's enthalpy of sorption with the volume fraction of carbon dioxide is nonmonotonic, following a trend similar to the one reported for the enthalpy of solvation of inert gases in water + alcohol mixtures [63–65,69]. Initially, $\Delta H_{S,et}^{\Phi}$ increases rapidly with Φ_{cd}, reaching a maximum around $\Phi_{cd} = 0.01$. Further increases in Φ_{cd} lead to a reduction in $\Delta H_{S,et}^{\Phi}$, which becomes even lower than the pure-gas value at $\Phi_{cd} = 0.06$. Thus, in the limit of infinite dilution, the presence of carbon dioxide initially renders ethane sorption less exothermic than in pure-gas sorption. Even though a change in the sign of $\Delta H_{S,et}^{\Phi}$ is not observed, this effect is still quite pronounced: the maximum value of $\Delta H_{S,et}^{\Phi}$ at about $\Phi_{cd} = 0.01$ is less than half the pure-gas value.

One possible explanation for the maximum in $\Delta H_{S,et}^{\Phi}$ would be a competition between the two gases for interacting with the polymer. In the presence of CO_2, ethane dissolution is likely to involve the rupture of some CO_2-polymer interactions to establish ethane–polymer interactions, a process that may not be energetically favored, since only CO_2 is thought to exhibit specific interactions with the ether groups in PEO (from Fig. 11, pure-gas CO_2 sorption is more exothermic than pure-gas C_2H_6 sorption). As the concentration of CO_2 in the polymer increases, a higher number of CO_2-polymer interactions must be broken to dissolve ethane and, therefore, a higher (less exothermic) $\Delta H_{S,et}^{\Phi}$ is observed. This competition between carbon dioxide and ethane for interaction

with the PEO backbone could be the reason for the minimum in mixed-gas ethane solubility.

As previously mentioned, there are two terms that contribute to the enthalpy of sorption. Only gas–polymer interactions were considered to explain the existence of the maximum in $\Delta H_{S,et}^{\Phi}$. The reduction in $\Delta H_{S,et}^{\Phi}$ with increasing carbon dioxide content in the polymer for $\Phi_{cd} > 0.01$ could be a result of a less endothermic contribution to create a cavity in the polymer matrix to accommodate ethane. As shown in Section 4.1, pure-gas ethane sorption is associated with the lowest polymer dilation, whose value at a given pressure increases considerably with the CO_2 mole fraction in the gas phase. Therefore, as a result of the polymer dilation brought about by the preferential dissolution of carbon dioxide in the polymer, the entropic cost of inserting ethane into the matrix is reduced compared to its pure-gas value. In other words, there is a higher probability of finding a cavity large enough to accommodate ethane in a polymer swollen with carbon dioxide. This would explain the increase in mixed-gas ethane solubility with increasing concentration of carbon dioxide dissolved in the polymer observed in Figs. 8 and 9. Once gain, results from molecular dynamics simulation would be helpful to further understand such phenomena.

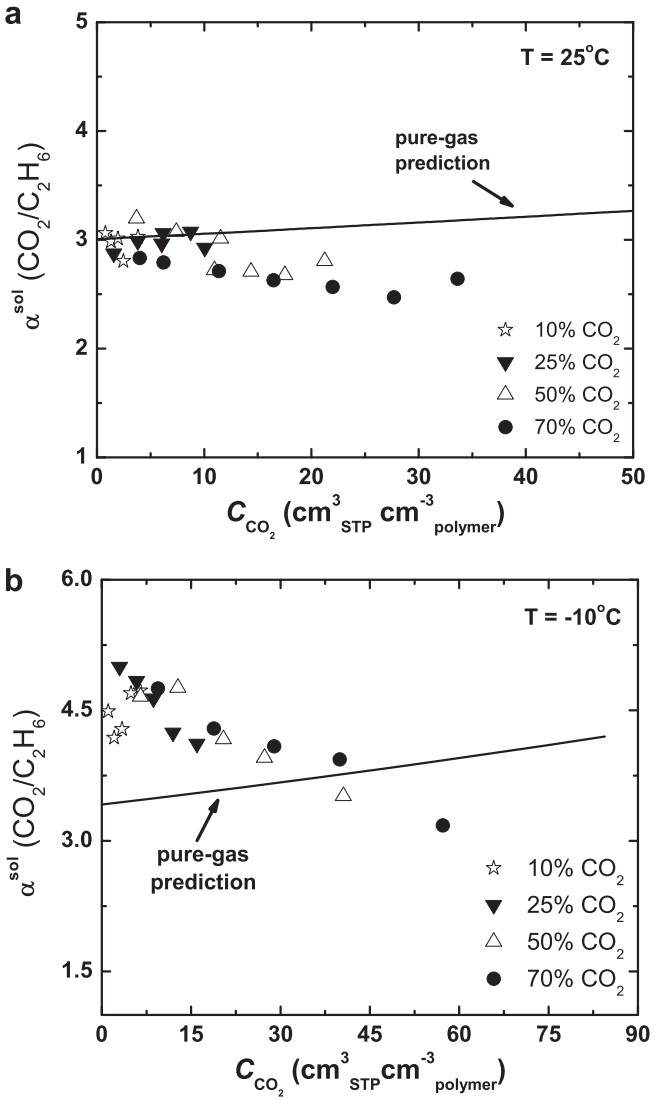

Fig. 12. Mixed-gas solubility selectivity (α^{sol}) of XLPEO copolymer at (a) 25 and (b) −10 °C as a function of the concentration of carbon dioxide dissolved in the polymer. Data are labeled according to the initial composition (in mol%) of the mixture that was in the charge volume (V_1 in Fig. 1). The lines are the pure-gas predictions from the Flory–Huggins model [15].

4.2.5. Solubility selectivity

We now consider the solubility selectivity ($\alpha_{ij}^{sol} = S_i/S_j$) of the XLPEO copolymer for CO_2 over C_2H_6, comparing the values obtained in the mixed-gas experiments with those predicted from pure-gas data. This comparison is presented in Fig. 12 for 25 °C and −10 °C, with mixed-gas solubility selectivity values plotted as a function of the equilibrium concentration of carbon dioxide dissolved in the polymer. The data for the other temperatures considered in this work can be found in the Supplementary Material.

At 25 °C, pure-gas estimations agree with the experimental values for mixtures when the amount of CO_2 dissolved in the polymer is small. However, the mixed-gas solubility selectivity decreases with increasing CO_2 content in the polymer, contrary to the increase predicted based on pure-gas data, and deviations between pure-(ideal) and mixed-gas(real) solubility selectivity values become significant at higher CO_2 concentrations. Similar trends are observed at 35 °C, as shown in the Supplementary Material.

A new aspect is revealed at $T \leq 0$ °C, as exemplified in Fig. 12(b) by the data at $T = -10$ °C. Due to the initial decrease in ethane solubility in the presence of CO_2 (Fig. 9), the mixed-gas solubility selectivity initially increases with increasing CO_2 concentration in the polymer, reaching a maximum, after which the decreasing trend already observed at higher temperatures is repeated. This maximum in mixed-gas α^{sol} is in good agreement with the minimum in ethane solubility in Fig. 9. In this case, there is always an initial range of CO_2 concentration in the polymer for which the solubility selectivity predicted based on the pure-gas data is actually lower than the mixed-gas value. The lower the operating temperature, the larger the extent of such region. In a forthcoming study, we explore whether this increase in solubility selectivity leads to increases in mixed-gas permeability selectivity.

5. Conclusions

In contrast to the general hypothesis that penetrants sorb independently in rubbery polymers, significant differences between pure- and mixed-gas solubility are found for carbon dioxide and ethane in a cross-linked poly(ethylene oxide) rubber prepared from photopolymerization of a 30 wt.% PEGDA–70 wt.% PEGMEA solution. Carbon dioxide, preferentially dissolved in the polymer due to its specific interactions with the ether groups in the polymeric chain, has its solubility at a given fugacity increased by the presence of ethane in the gas phase, an effect that becomes more pronounced as the operating temperature is reduced or the ethane activity in the gas mixture increases. At $T \geq 25$ °C, ethane solubility also increases in the presence of carbon dioxide. However, at $T \leq 0$ °C, the change in ethane solubility as a function of the amount of CO_2 dissolved in the polymer is nonmonotonic, with the existence of a minimum at low CO_2 concentrations. In general, ethane solubility can be reduced, increased or even remain unchanged in the presence of carbon dioxide, depending on the operating temperature and on the activity of CO_2 in the gas phase. As a result, the solubility selectivity of the polymer in equilibrium with a carbon dioxide/ethane mixture is a complex function of the operating conditions (pressure, temperature, and mixture composition), and it can be either higher or lower than the value estimated from pure-gas data.

The multicomponent Flory–Huggins model with fitted interaction parameters can represent both the pure- and the mixed-gas sorption isotherms well for this system, with experimentally determined partial molar volumes of each gas in the polymer. All

interaction parameters are temperature-dependent, and for $T \leq 0$ °C, an empirical composition dependence is required to properly represent the data.

In the limit of infinite dilution, the isosteric enthalpy of sorption of both carbon dioxide and ethane is a function of the volume fraction of the other species in the polymeric solution. For carbon dioxide, the sorption process is always more exothermic in the presence of ethane, whereas pure-gas ethane sorption is usually more exothermic than ethane sorption in the presence of CO_2. Thus, the interaction of carbon dioxide with the ethylene oxide units in this polymer is favored by the presence of ethane.

Acknowledgments

The authors would like to express their thanks to Professor N.F.A. van der Vegt, from the Technical University of Darmstadt (Germany), for helpful discussions regarding the thermodynamics of gas dissolution. One of the authors (C. P. Ribeiro) would like to thank the Brazilian Agency CAPES for their financial support (Grant 2458/07-1). The authors also gratefully acknowledge partial support of this work by the U.S. Department of Energy (Grant DE-FG02-02ER15362) and by the U.S. National Science Foundation (Grant IIP-0917971). A portion of this research is based upon work supported by the U.S. National Science Foundation under Grant No. DMR #0423914.

Nomenclature

a	activity
C	concentration of gas dissolved in the polymer
c_{0-5}	empirical coefficients in Eq. (7)
f	fugacity
l_0	length of the polymer sample under vacuum at the operating temperature
m	volume fraction in the binary system
P	pressure
R	universal gas constant
S	gas solubility in the polymer
S^{PG}_{max}	highest pure-gas solubility measured at a given temperature
S^{PG}_{min}	lowest pure-gas solubility measured at a given temperature
T	temperature
V_0	volume of the degassed polymer sample at the operating temperature
V_n	volume of the polymer sample at the operating temperature and a pressure P_n
$\overline{V}$	partial molar volume
y	mole fraction in the binary system

Greek letters

α^{sol}	solubility selectivity
β^{∞}, β^{*}	empirical parameters in Eq. (8b)
χ	Flory–Huggins interaction parameter
δ^{∞}, δ^{*}	empirical parameters in Eq. (8a)
ΔG^E	excess Gibbs energy of mixing
ΔH_S	enthalpy of sorption
ΔL	change in the length of the polymer sample
Δu_{vv}	solvent reorganization energy
Δu_{uv}	penetrant-polymer interaction energy
ΔV	change in the polymer volume
γ^{∞} γ^{*}	empirical parameters in Eq. (8c)
Ω	Ostwald solubility coefficient
Φ	volume fraction

Subscripts

3	polymer
∞	infinite dilution
cd	carbon dioxide
et	ethane
i	component i

Superscripts

°	value at standard condition
^	property in the mixture
Φ	isosteric value
sat	saturation

Appendix. Supplementary material

Supplementary data associated with this article can be found, in the online version, at doi:10.1016/j.polymer.2010.01.012.

References

[1] Powell CE, Qiao GG. J Membr Sci 2006;279:1–49.
[2] Sridhar S, Smitha B, Aminabhavi TM. Sep Purif Rev 2007;36:113–74.
[3] Hirayama Y, Kase Y, Tanihara N, Sumiyama Y, Kusuki Y, Haraya K. J Membr Sci 1999;160:87–99.
[4] Lin H, van Wagner E, Raharjo R, Freeman BD, Roman I. Adv Mater 2006;18:39–44.
[5] Lin H, van Wagner E, Freeman BD, Toy LG, Gupta RP. Science 2006;311:639–42.
[6] Kusuma VA, Freeman BD, Jose-Yacaman M, Lin H, Kalakkunnath S, Kalika DS. Structure/property characteristics of polar rubbery membranes for carbon dioxide removal. In: Li NN, Fane AG, Ho WSW, Matsuura T, editors. Advanced membrane technology and applications. Hoboken: Wiley; 2008. p. 929–53.
[7] Kusuma VA, Freeman BD, Borns MA, Kalika DS. J Membr Sci 2009;327:195–207.
[8] Kusuma VA, Matteucci S, Freeman BD, Danquah MK, Kalika DS. J Membr Sci 2009;341:84–95.
[9] Lin H, van Wagner E, Swinnea JS, Freeman BD, Pas SJ, Hill AJ, et al. J Membr Sci 2006;276:145–61.
[10] Kelman S, Lin H, Sanders ES, Freeman BD. J Membr Sci 2007;305:57–68.
[11] Lin H, Kai T, Freeman BD, Kalakkunnath S, Kalika DS. Macromolecules 2005;38:8381–93.
[12] Lin H, Freeman BD. Macromolecules 2005;38:8394–407.
[13] Raharjo RD, Lin H, Sanders DF, Freeman BD, Kalakkunnath S, Kalika DS. J Membr Sci 2006;283:253–65.
[14] Ribeiro CP, Freeman BD. Macromolecules 2008;41:9458–68.
[15] Ribeiro CP, Freeman BD. J Polym Sci Part B Polym Phys 2010;48:456–68.
[16] Joffrion LL, Glover CJ. Macromolecules 1986;19:1710–8.
[17] Ruff WA, Glover CJ, Watson AT, Lau WR, Holster JC. AIChE J 1986;32:1954–62.
[18] Surana RK, Danner RP, Duda JL. Ind Eng Chem Res 1998;37:3203–7.
[19] Schabel W, Scharfer P, Kind M, Mamaliga I. Chem Eng Sci 2007;62:2254–66.
[20] Raharjo RD, Freeman BD, Sanders ES. J Membr Sci 2007;292:45–61.
[21] Lue SJ, Wu SY, Wang SF, Wang LD, Tsai CL. Desalination 2008;233:286–94.
[22] Yurekli Y, Altinkaya SA. Fluid Phase Equilibria 2009;277:35–41.
[23] Zielinski JM, Fry R, Kimak MF. Macromolecules 2004;37:10134–40.
[24] Jones AT, Danner RP, Duda JL. J Appl Polym Sci 2008;110:1632–41.
[25] Koros WJ, Chern RT, Stannett VT, Hopfenberg HB. J Polym Sci Polym Phys Ed 1981;19:1513–30.
[26] Lin H, Freeman BD. J Membr Sci 2004;239:105–17.
[27] Lin H, Freeman BD. J Mol Struct 2005;739:57–74.
[28] Gall GH, Sanders ES. Oil Gas J 2002;100:48–55.
[29] Nordstad KH, Kristiansen TK, Dortmundt D. Hybrid separation of CO_2 from ethane using membranes. In: Proceedings of the 53rd LRGCC conference; 2003. p. 251–8.
[30] Liley PE, Thompson GH, Friend DG, Daubert TE, Buck E. Physical and chemical data. In: Perry RH, Green DW, editors. Perry's chemical engineer's handbook. 7th ed. New York: McGraw-Hill Professional; 1997. pp. 2–1–2–374.
[31] Lindvig T, Economou IG, Danner RP, Michelsen ML, Kontogeorgis GM. Fluid Phase Equilibria 2004;220:11–20.
[32] Flory PJ. Principles of polymer chemistry. Ithaca: Cornell University Press; 1953.
[33] Mulder MHV, Smolders CA. J Membr Sci 1984;17:289–307.
[34] Allcock HR, Lampe FW, Mark JE. Contemporary polymer chemistry. 3rd ed. Upper Saddle River: Pearson Education; 2003.
[35] Lipnizki F, Trägardh G. Sep Purif Methods 2001;30:49–125.
[36] Lindvig T, Michelsen ML, Kontogeorgis GM. Fluid Phase Equilibria 2002;203:247–60.
[37] Kalakkunnath S, Kalika DS, Lin H, Freeman BD. Macromolecules 2005;38:9679–87.
[38] Burnett ES. J Appl Mech 1936;3:136–40.
[39] Koros WJ, Paul DR. J Polym Sci Polym Phys Ed 1976;14:1903–7.

[40] Lin H, Freeman BD. Permeation and diffusion. In: Czichos H, Saito T, Smith L, editors. Springer handbook of materials measurement methods. Leipzig: Springer; 2006. p. 371–97.
[41] Van Ness HC, Abbott MM. Thermodynamics. In: Perry RH, Green DW, editors. Perry's chemical engineer's handbook. 7th ed. New York: McGraw-Hill Professional; 1997. 4–19–4–20.
[42] Koros WJ, Paul DR, Rocha AA. J Polym Sci Polym Phys Ed 1976;14: 687–702.
[43] Dymond JH, Marsh KN, Wilhoit RC, Wong KC. The virial coefficients of pure gases and mixtures. Darmstadt: Springer; 2001.
[44] Sherman GJ, Magee JW, Ely JF. Int J Thermophys 1989;10:47–59.
[45] Brugge HB, Hwang C-A, Rogers WJ, Holste JC, Hall KR, Lemming W, et al. Physica A 1989;156:382–416.
[46] J.M.,Humphreys AE. The GERG databank of high accuracy compressibility factor measurements, Tech. rep., GERG technical monograph 4, http://www.gerg.info/publications/tm.htm; 1990.
[47] McElroy PJ, Dowd MK, Battino R. J Chem Thermodyn 1990;22:505–12.
[48] Weber LA. Int J Thermophys 1992;13:1011–32.
[49] Raharjo RD, Freeman BD, Sanders ES. Polymer 2007;48:6097–114.
[50] Sanders E, Koros W, Hopfenberg H, Stannett V. J Membr Sci 1984;18: 53–74.
[51] Schuld N, Wolf BA. Polymer-solvent interaction parameters. In: Brandrup J, Immergut EH, Grulke EA, editors. Polymer handbook. 4th ed. New York: John Wiley & Sons; 1999. p. VII247–64.
[52] Anderson TF, Abrams DS, Grens EA. AIChE J 1978;24:20–9.
[53] O'Connell JP, Prausnitz JM. Ind Eng Chem Fundam 1964;3:347–51.
[54] O'Connell JP. AIChE J 1971;17:658–63.
[55] Rudolph ESJ, Zomerdijk M, Ottens M, van der Wielen LAM. Ind Eng Chem Res 2001;40:398–406.
[56] Mainar AM, Pardo JI, Santafe J, Urieta JS. Ind Eng Chem Res 2003;42:1439–50.
[57] Ellegaard ME, Abildskov J, O'Connell JP. AIChE J 2009;55:1256–64.
[58] Davalos J, Anderson WR, Phelps RE, Kidnay AJ. J Chem Eng Data 1976;21:81–4.
[59] Brown TS, Kidnay AJ, Sloan ED. Fluid Phase Equilibria 1988;40:169–84.
[60] Wei MSW, Brown TS, Kidnay AJ, Sloan ED. J Chem Eng Data 1995;40:726–31.
[61] Fredenslund A, Mollerup J. J Chem Soc Faraday Trans 1974;70:1653–60.
[62] Ben-Naim A, Baer S. J Chem Soc Faraday Trans 1964;60:1736–41.
[63] Cargill RW, Morrison TJ. J Chem Soc Faraday Trans 1975;71:618–24.
[64] Cargill RW. J Chem Soc Faraday Trans 1976;72:2296–300.
[65] Cargill RW. J Chem Soc Faraday Trans 1978;74:1444–56.
[66] Ben-Naim A, Phys J. Chem 1965;69:3240–5.
[67] van der Vegt NFA, Trzesniak D, Kasumaj B, van Gunsteren WF. Chem Phys Chem 2004;5:144–7.
[68] Özal TA, van der Vegt NFA. J Phys Chem B 2006;110:12104–12.
[69] Lee ME, van der Vegt NFA. J Chem Theory Comput 2007;3:194–200.
[70] Matteucci S, Yampolskii Y, Freeman BD, Pinnau I. Transport of gases and vapors in glassy and rubbery polymers. In: Yampolskii Y, Pinnau I, Freeman BD, editors. Materials science of membranes for gas and vapor separation. New York: John Wiley & Sons; 2006. p. 1–47.
[71] van der Vegt NFA. J Membr Sci 2002;205:125–39.
[72] van der Vegt NFA. New perspectives of gas sorption in solution-diffusion membranes. In: Pinnau I, Freeman BD, editors. Advanced materials for membrane separations. Washington: ACS; 2004. p. 39–54.
[73] van der Vegt NFA, Briels WJ, Wessling M, Strathmann H. J Chem Phys 1996;105:8849–57.